

Chemo-Mechanically Regulated Oscillation of an Enzymatic Reaction

Ximin He,[†] Ronn S. Friedlander,^{||} Lauren D. Zarzar,[‡] and Joanna Aizenberg^{*,†,§,‡}[†]School of Engineering and Applied Sciences, [‡]Department of Chemistry and Chemical Biology, and [§]Kavli Institute for Bionano Science and Technology at Harvard University, Harvard University, Cambridge, Massachusetts 02138, United States^{||}Harvard-MIT Division of Health Sciences and Technology, Cambridge, Massachusetts 02139, United States**S** Supporting Information**KEYWORDS:** responsive material, chemo-mechanical, oscillation, enzymatic reaction

A necessity of all living organisms from prokaryotes to mammals is the capability to respond rapidly to a changing environment via a variety of adaptive mechanisms. At the core of this adaptive nature are hierarchical signaling cascades that allow the organism to transform a stimulus signal into a variety of outputs—often visible or otherwise detectable readouts (color change, movement, etc.).¹ Essential to these functions are sophisticated receptors that freely transduce chemical and mechanical as well as other types of energy. These mechanochemical interconversions occur at various length scales, from the nanoscale (e.g., ribosomal procession along an mRNA strand, F1-ATPase)² to the microscale (e.g., flagellar motors, hair cells)^{3,4} and even the macroscale (e.g., muscle movement by myocyte action).⁵

In contrast to nature's highly integrated and versatile cascades allowing transitions between biochemical and mechanical processes, our current synthetic world has few materials systems (e.g., responsive microfluidic valves)⁶ that integrate mechano-chemical ($M \rightarrow C$) transductions (e.g., sensors)^{7,8} with chemo-mechanical ($C \rightarrow M$) ones (e.g., actuators),^{9–12} thereby enabling coupling between these two types of energy with various outputs ($C_1 \rightarrow M \rightarrow C_2 \rightarrow \text{output}$).^{13,14} More importantly, existing synthetic systems are generally incapable of hierarchically amplifying signals arising from the molecular level to give macroscopic readouts that are easily detectable, which is a highly desired property of next-generation materials,^{15,16} as well as biosensing and analytical devices.¹⁷ Incorporating a sophisticated biological process into materials and larger hierarchical systems presents a challenge and requires a broad-based design capable of mediating a large repertoire of biochemical processes.

The numerous biological examples of chemo-mechanical transduction and transformation show us that nature's bottom-up approach to the assembly of functional structures relies upon hierarchical ordering of molecular and cellular subunits through compartmentalization.¹⁸ It is via the coordinated activities of constituent parts that molecular-scale events can trigger macro-scale responses, such as the expansion and contraction of cephalopod chromatophores that determine the organism's overall apparent color pattern¹⁹ and ATP-driven muscle contraction.⁵ Inspired by these and other similar phenomena, we have recently developed self-regulated mechano-chemical adaptively reconfigurable tunable systems (SMARTS),¹³ which offer smooth coupling and coordination

of microscopic and macroscopic signals with fast mechanical action and a diverse range of chemical inputs and outputs. By embedding the catalyst-bearing “skeletal” microstructures into a pH- or temperature-responsive hydrogel “muscle” and introducing a fluid containing reactive “nutrients”, we created a platform that allowed us to precisely control a number of externally regulated $C_1 \rightarrow M \rightarrow C_2$ systems, such as pulsed gas generation and dynamic fluorescence quenching. Incorporation of carefully designed feedback mechanisms ($C \rightleftharpoons M$) into these systems has enabled continuous chemical, thermal, and mechanical energy interconversions, resulting in autonomous, self-sustained dynamic materials.

Biochemical reactions, if integrated with the highly tunable and customizable SMARTS, would open doors to the control of innumerable sophisticated, environmentally friendly, enzymatic, or other biological activities useful for self-regulating medical implants, such as biomolecule detection, separation, and signal amplification. Biochemical processes in general are typically sensitive to pH, temperature, and salt concentrations, requiring a narrow range to operate successfully. Therefore, we aimed to tailor SMARTS to function in delicate, biologically relevant environments in order for it to be ultimately capable of regulating complex, multicomponent biochemical processes. This would greatly expand the scope of SMARTS and demonstrate the utility of this broad-based platform for biomedical applications and biological studies. Specifically, the exquisite controllability provided by SMARTS, which enables the transport of biomolecules between distinct aqueous environments via microstructure actuation, allows for externally regulated, oscillating biochemical reactions with programmable cycles and outputs. Here, we demonstrate chemo-mechanically mediated cyclic “on–off” switching of an exemplary enzymatic reaction—the luciferase (LUC)-catalyzed oxidation of luciferin using SMARTS. In this system, we convert pH changes to mechanical movement which in turn triggers a biochemical reaction that generates light. In this way we create a signal cascade/converter capable of translating signals at the nanoscale to outputs that can be visualized at the macroscale.

Our system is composed of an array of epoxy microfins embedded in pH-sensitive hydrogel and immersed in an

Received: October 13, 2012

Revised: January 20, 2013

aqueous bilayer formed in a microfluidic channel (Figure 1a,b). To generate the microfins, silicon masters with a staggered

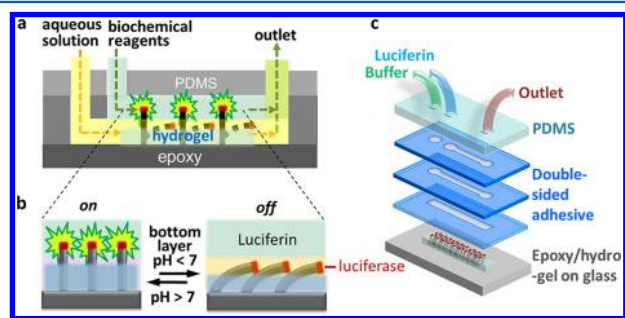
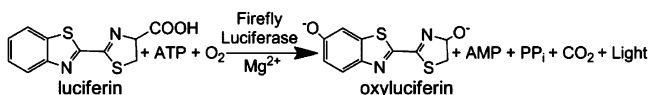


Figure 1. Fabrication of the oscillating bioluminescence reactor. a. Side-view schematic of oscillations in a bioluminescence-generating enzymatic reaction triggered by pH, using a pH-responsive gel to actuate epoxy microstructures immersed in an aqueous bilayer in a microfluidic device. b. Close-up schematic showing the reversible chemo-mechanical “on–off” switching of bioluminescence-generating luciferin oxidation by the enzyme LUC. c. Schematic of the fabrication of the microfluidic device that allows forming an aqueous bilayer. A polyacrylic double-sided adhesive tape stack with a rectangular channel and two vertically separated inlets and one outlet was placed on top of the microfins and served as the walls of the channel, which was sealed by a PDMS sheet, with inlet and outlet tubings connected to it.

array of microfins (each fin being 2 μm wide, 10 μm long, and 18 μm tall) was replicated in epoxy (9:1 (w/w) UVO-114 (Epoxy technology):glycidyl methacrylate) (see Supporting Information for details). To embed microfin structures into a hydrogel film, a drop of hydrogel precursor solution was placed on the freshly prepared microfin surface and was cured under broadband UV illumination (see Supporting Information for details). Because of the instability of the enzyme LUC outside of the pH range of 6.0–9.0, we tuned the volume phase transition pH of the hydrogel poly(acrylamide-*co*-acrylic acid)²⁰ from pH 4.3 to pH 7, by introducing 10% (w/v) dodecyl acrylate comonomer to the precursor pH-responsive hydrogel solution.²¹

For the cyclic enzymatic reaction, fin tips were functionalized with LUC (Supporting Information Figure S1). The localization of LUC to the fin tips allowed for movement of the catalyst between the two aqueous layers using the SMARTS system (Figure 1a,b). LUC catalyzes the oxidation of luciferin to generate light via the following reaction:



An aqueous solution of D-luciferin sodium salt, MgCl_2 , and ATP magnesium salt in HEPES pH 7.5 buffer was used in the top fluid layer as the reagent medium. The reagent solution was oxygenated, and the O_2 -permeable PDMS channel allowed further diffusion of O_2 for the oxidation reaction.

To create a vertically separated aqueous bilayer, a microfluidic channel with two inlets of different depths was fabricated on top of the hydrogel-embedded microfins (Figure 1c). Reagent solution and water were flowed into the two inlets, creating a laminar flow interface that passed below the tips of the microfins. The bottom fluid was an alternating flow of pH 6.0 sodium citrate and pH 9.0 sodium tetraborate buffers to induce expansion and contraction of the hydrogel, thereby driving the microfin actuation.

Microscopic fluorescence imaging and video recording were done using a confocal microscope equipped with an avalanche photodiode detector (APD) for quantification of the light emission. We simultaneously recorded the macroscopic dynamic processes while the microscopic videos and images were taken, as seen in Movie 1 (Supporting Information) and Figure 2. The intensity of the reaction-generated luminescence

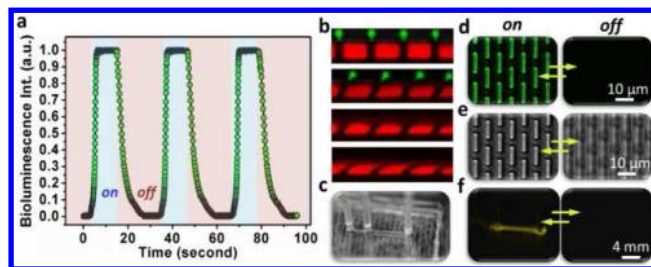


Figure 2. Dynamic light emission shown at the macro- and microscale by a mechanically controlled bioluminescence reaction in SMARTS. a. Oscillations in bioluminescence intensity from controlled LUC-catalyzed luciferin oxidation synchronous with the oscillating movement of the LUC-functionalized microfins driven by the expansion and contraction of the pH-responsive gel resulting from alternating flow of the buffers at pH 6 (pink) and 9 (blue) through the microfluidic device. b. XZ sections of fins at various stages of actuation. Images are overlays of two emission channels: red, rhodamine-conjugated hydrogel; green, luminescent emission from the luciferin oxidation reaction. c. Digital camera photo of the microfluidic device. d. Confocal micrographs of microfins with luminescence on/off recorded without exogenous light. e. Transmitted light micrographs, revealing the configuration of bent microfins without bioluminescence. f. Digital camera photos of the microfluidic device without exogenous light, showing the macroscopic effect.

was measured from each focal plane containing fin tips recorded with the APD. Figure 2a shows the periodic change in the emitted light intensity during the microfin actuation; light intensity increases sharply as the fins stand upright with the flow of a pH 9 buffer in the bottom layer, and the intensity quickly decreases as the tips bend down with the flow of pH 6 buffer in the bottom layer. We attribute the observed bioluminescence without the typical “flash” behavior²² for the reaction to the flow system, which prevented the accumulation of oxyluciferin and dehydroluciferin-adenylate and thus the inhibition of enzyme.²³ The observed luminescence decay in the “off” phase perhaps resulted from the residual oxyluciferin or a small quantity of luciferin remaining on the tips across the interface. The rapid responsiveness and precise synchronization of the light emission and the microfin movement in and out of the reagent layer during multiple cycles are well evidenced by the time-resolved bioluminescence intensity in Figure 2a and Movie 1 (Supporting Information). Side-view configuration images of SMARTS using confocal XZT scanning and fluorescently labeled hydrogel (Figure 2b) clearly reveal the dynamics of luminescence generation on fin tips during all stages of actuation (Supporting Information Figure S3). The microscope images in Figure 2d display the “on” and “off” states of light emission correlated to the upright or bent configurations of the fins. The microfin actuation was also recorded in transmission mode (Figure 2e) to reveal the structures’ configuration during the bent state (without light emission from bioluminescence). A series of control reactions conducted at pH 6, 7.5, and 9 in a static system (Supporting Information Figure S2) emitted light without appreciable

changes in intensity, indicating that luminescence is not lost due to pH changes within the operating pH range. This confirmed that the disappearance of luminescence at pH 6 resulted from the cessation of the reaction due to the tips bending away from top reagent layer rather than from the quenching of luminescence or dysfunction of the enzyme. The proper function of the enzyme is further supported by the sustained luminescence through 30–40 actuation cycles. Importantly, intermittent light emission was also apparent macroscopically: in the channel of the microfluidic device shown in Figure 2c, visible readouts arising from the periodic bioluminescent reaction were detected (Figure 2f).

The precise and swift on/off switching of the bioluminescent reaction (Supporting Information Figure S3) demonstrates the excellent coordination of the chemically induced mechanical motion ($C_1 \rightarrow M$) with the mechanically modulated enzymatic activity ($M \rightarrow C_2$). Using periodic changes in pH in the bottom layer as the stimulus, we realized a synchronous cascade of chemo-mechano-(bio)chemical light generation cycles. Through pH-mediated swelling of the hydrogel “muscle”, the coordinated bending of tens of thousands of catalyst-decorated microfins generated light in the top fluid layer visible to the naked eye. The multiscale cascade provides readouts of unrelated but coupled chemical events (i.e., pH change to light emission) and can be used to arbitrarily couple a vast range of reactions.

In summary, we have demonstrated precise control of biochemical signal transduction using a model system composed of LUC bound to microstructure tips, catalyzing the oxidation of luciferin in an oscillatory fashion. The SMARTS device is shown to be both compatible with delicate biological constraints and capable of accommodating enzymatic reactions for signal transduction, attributed to its modularity, tunability, and physical simplicity. Moreover, the hybrid hydrogel-microstructured surface is well integrated in a microfluidic channel, showing that this chemo-mechanical system can be readily applied in microfluidic lab-on-a-chip systems to create effective, complex, and highly integrated microfluidic networks for automated biological processes.²² The potential variety of switchable biochemical reactions that could be accommodated by this $C_1 \rightarrow M \rightarrow C_2$ cascade is complemented by the customizability of the hydrogel response, which can, in turn, be tailored to a wide range of stimuli, such as pH, heat, light, glucose, or other metabolic compounds, as well as the vast varieties of outputs, such as gas generation, color change, DNA polymerization, and proteolysis, thus improving the combinatorial diversity of coupled effects. This work demonstrates an important step toward biomimetic, responsive materials and should pave the way for more applications in microfluidic and biosensor systems, such as in-line sensors with novel readouts and outputs.

■ ASSOCIATED CONTENT

📄 Supporting Information

I, Methods and Characterization; II, Control study of pH effect on the bioluminescence; and III, Study of modulation process of the biochemical processes via the mechanical motion. A movie. This material is available free of charge via the Internet at <http://pubs.acs.org>.

■ AUTHOR INFORMATION

Corresponding Author

*E-mail: jaiz@seas.harvard.edu.

Notes

The authors declare no competing financial interest.

■ ACKNOWLEDGMENTS

The authors thank M. Aizenberg for valuable advice on this work and help with manuscript preparation and A. Ehrlicher and T. Kodger for technical assistance with luminescence imaging using a confocal microscope. This work was supported by the US DOE under Award No. DE-SC0005247.

■ REFERENCES

- (1) Prosser, B. L.; Ward, C. W.; Lederer, W. J. *Science* **2011**, *333*, 1440.
- (2) Sambongi, Y.; Iko, Y.; Tanabe, M.; Omote, H.; Iwamoto-Kihara, A.; Ueda, I.; Yanagida, T.; Wada, Y.; Futai, M. *Science* **1999**, *286*, 1722.
- (3) Berg, H. C. *Annu. Rev. Biochem.* **2003**, *72*, 19.
- (4) Fettilplace, R.; Hackney, C. M. *Nat. Rev. Neurosci.* **2006**, *7*, 19.
- (5) Hess, H. *Annu. Rev. Biomed. Eng.* **2011**, *13*, 429.
- (6) Beebe, D. J.; Moore, J. S.; Bauer, J. M.; Yu, Q.; Liu, R. H.; Devadoss, C.; Jo, B.-H. *Nature* **2000**, *404*, 288.
- (7) Ariga, K.; Mori, T.; Hill, J. P. *Chem. Sci.* **2011**, *2*, 195.
- (8) Todres, Z. V. *Organic mechanochemistry and its practical applications*; CRC/Taylor & Francis: 2006.
- (9) Lahann, J.; Langer, R. *MRS Bull.* **2005**, *30*, 185.
- (10) He, X. M.; Li, C.; Chen, F. G.; Shi, G. Q. *Adv. Funct. Mater.* **2007**, *17*, 2911.
- (11) Sidorenko, A.; Krupenkin, T.; Taylor, A.; Fratzl, P.; Aizenberg, J. *Science* **2007**, *315*, 487.
- (12) Paxton, W. F.; Sundararajan, S.; Mallouk, T. E.; Sen, A. *Angew. Chem., Int. Ed.* **2006**, *45*, 5420.
- (13) He, X.; Aizenberg, M.; Kuksenok, O.; Zarzar, L. D.; Shastri, A.; Balazs, A. C.; Aizenberg, J. *Nature* **2012**, *487*, 214.
- (14) Fratzl, P.; Barth, F. G. *Nature* **2009**, *462*, 442.
- (15) Stuart, M. A. C.; Huck, W. T. S.; Genzer, J.; Muller, M.; Ober, C.; Stamm, M.; Sukhorukov, G. B.; Szleifer, I.; Tsukruk, V. V.; Urban, M.; Winnik, F.; Zauscher, S.; Luzinov, I.; Minko, S. *Nat. Mater.* **2010**, *9*, 101.
- (16) Kim, P.; Zarzar, L. D.; He, X. M.; Grinthal, A.; Aizenberg, J. *Curr. Opin. Solid State Mater. Sci.* **2011**, *15*, 236.
- (17) Li, D. B.; Paxton, W. F.; Baughman, R. H.; Huang, T. J.; Stoddart, J. F.; Weiss, P. S. *MRS Bull.* **2009**, *34*, 671.
- (18) Koga, S.; Williams, D. S.; Perriman, A.; Mann, S. *Nat. Chem.* **2011**, *3*, 720.
- (19) Mathger, L. M.; Denton, E. J.; Marshall, N. J.; Hanlon, R. T. *J. R. Soc., Interface* **2009**, *6*, S149.
- (20) Richter, A.; Paschew, G.; Klatt, S.; Lienig, J.; Arndt, K. F.; Adler, H. J. P. *Sensors* **2008**, *8*, 561.
- (21) Philippova, O. E.; Hourdet, D.; Audebert, R.; Khokhlov, A. R. *Macromolecules* **1997**, *30*, 8278.
- (22) DeLuca, M.; McElroy, W. *Biochemistry* **1974**, *13*, 921.
- (23) Ribeiro, C.; Esteves da Silva, J. C. G. *Photochem. Photobiol. Sci.* **2008**, *7*, 1085.
- (24) Melin, J.; Quake, S. R. *Annu. Rev. Biophys. Biomol. Struct.* **2007**, *36*, 213.